

# AGENT-BASED MODELING OF MEMS FLUIDIC SELF-ASSEMBLY

Massimo Mastrangeli<sup>1,2</sup>, Chris Van Hoof<sup>1,3</sup>, Rajashree Baskaran<sup>4</sup>, Jean-Pierre Celis<sup>2</sup>  
and Karl F. Böhringer<sup>5</sup>

<sup>1</sup>IMEC, Leuven (BE) <sup>2</sup>MTM, Katholieke Universiteit Leuven, Leuven (BE)

<sup>3</sup>ESAT, Katholieke Universiteit Leuven, Leuven (BE) <sup>4</sup>Intel Corp., Portland (USA)

<sup>5</sup>Electrical Engineering Dept., University of Washington, Seattle (USA)

## ABSTRACT

The dynamics of MEMS 3D fluidic self-assembly (FSA) was modeled using interactive software agents, *i.e.* by agent-based modeling (ABM). ABM enables realistic simulations of 3D FSA dynamics taking into account spatial parameters - hard to include in analytic models. Our ABM model was tested by reproducing the experimental data of Zheng and Jacobs's 3D FSA process, and it was used to investigate the influence of design parameters and assembly strategies on FSA yield. The ABM model is a significant advance in the modeling of FSA and may represent the natural framework to explore open issues in this promising field.

## 1. INTRODUCTION

Microscale self-assembly, featuring massive parallelism and contactless handling of devices, may complement, enhance and eventually replace established MEMS assembly techniques [1]. Particularly, fluidic self-assembly (FSA) exploits fluids for the mass transport and stochastic motion of devices in bounded assembly spaces, geometric shape-matching for selective device assembly and capillary forces for the electro-mechanical binding of devices. FSA was already adopted to assemble and to package microdevices onto several types of substrates [2-3] and into 3D functional units [4].

In general, SA comprises many different phenomena (*e.g.* physico-chemical, collective) that simultaneously influence its performance and thus should be considered in its modeling. A few analytic models of (F)SA processes were proposed in the literature [1, 5, 6]. Such models, though, are based on master equation formulations inspired by chemical kinetics, *i.e.* they lump all design and control parameters into reaction rates. By abstracting from the details, they may capture the average process dynamics, but they lack specificity. Importantly, they are based on rather simplifying assumptions such as, *e.g.*, reaction-limited processes, unbounded assembly spaces and point-like components [1]. Simulation is therefore the only option. However, on the one hand almost all attempts so far focused on quasi-static FEM modeling of single-component FSA physics [7]. FEM cannot properly capture SA dynamics because: 1) it typically acts at single-component level, excluding component interactions and related collective and stochastic phenomena; 2) it cannot easily handle systems with changing topologies (*e.g.* components that make and break contact). On the other hand, fully-stochastic (*e.g.* Monte Carlo) simulations [8] provide for a level of abstraction where spatial constraints and microscopic,

physical and geometrical details of the processes cannot be easily embedded [9].

Interestingly, agent-based modeling (ABM) – a well-understood methodology used for a wide range of applications [10] – can handle spatial constraints and describe the physics of multi-body interactions at the system level.

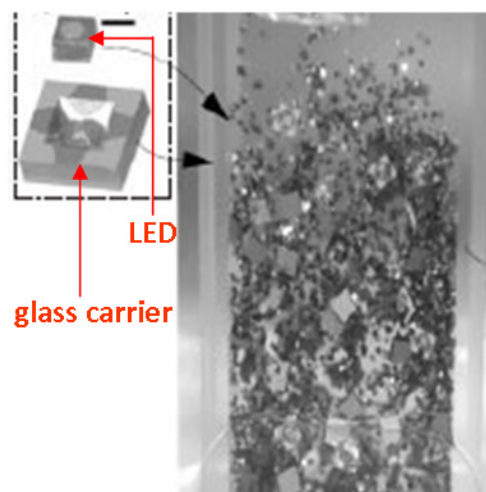


**Figure 1.** The 3D FSA process developed by Zheng and Jacobs [4]. LEDs stochastically assembled into shape-matching glass carriers, and were thereby retained by the capillary forces of molten solder. The same authors proposed a closed-form model of the process, which we recently generalized to include dis-assembly events [1]. (Illustration courtesy of H. O. Jacobs).

We hereby propose the modeling of MEMS FSA using software agents with pre-defined features, spatially moving and interacting according to programmable rules that encode physical laws and constraints. Finite component dimensions, bounded assembly spaces, diffusion-limited and stochastic collision dynamics among multiple components can straightforwardly be encoded in ABM models, which furthermore allow large freedom to implement realistic physical interactions. We illustrate our ABM 3D FSA model by reproducing the experimental data of Zheng and Jacobs' FSA process (Fig. 1) [4]. We then use the model to investigate the influence of several design parameters and assembly strategies on FSA yield, and finally to predict a possible history of a yet-unperformed FSA process involving 3 co-existing sets of components. Incidentally, our model may represent a 3D extension of the 2D microscopic model proposed by Mermoud [9].

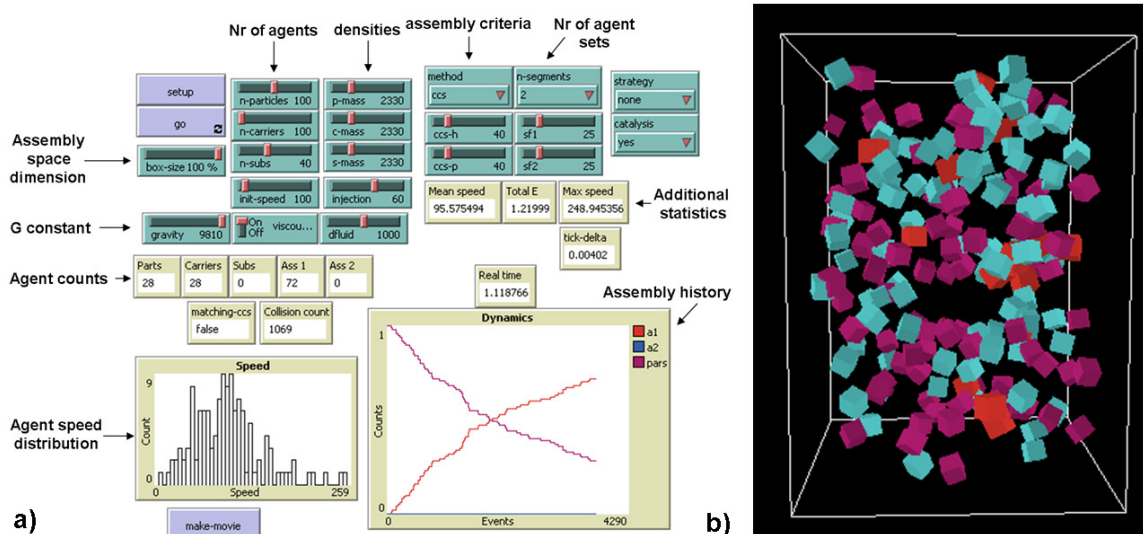


**Figure 2.** The customized NetLogo graphical interface of our 3D FSA agent-based model. **a)** Control parameters and real-time statistics, **b)** snapshot from a simulation of Zheng and Jacobs' 3D FSA process (compare with Fig. 1) between two sets of agents (magenta = LEDs, cyan = glass carriers) self-assembling into packaged (red) units by the MCCS criterion (illustrated in Fig. 3).

## 2. ABM OF 3D FSA PROCESSES

We developed our agent-based model of 3D FSA using NetLogo<sup>1</sup> (NL) [11]. Our customized interface is shown in Fig. 2. NL concurrently simulates the behavior of many interacting agents, as specified by programmable boundary conditions and interaction rules. NL allows controlling all roto-translational degrees of freedom and the instantaneous direction of movement of each agent. We could therefore define interaction rules that reproduced the geometry and physics of actual (F)SA processes. In our code the agents (*i.e.* the devices to be assembled) were defined in terms of number of sets and of agents of each set; and by the shape, volume, density and initial speed magnitude of each agent. Each agent's initial position and direction of motion was chosen randomly from uniform distributions; the initial speed magnitude was set equal for all agents. We defined the dimensions of the assembly space; and we implemented gravity, the fluidic drag (using the Stokes approximation for low Reynolds numbers) induced by the hosting fluid on the floating agents, and external energy injections to simulate agent stirring. We encoded elastic, hard-sphere 2-body collisions; and we defined 2 alternative criteria - either based on probability or on geometric conditions (described in Fig. 3) - for sterically-effective (*i.e.* leading to assembly) inter-agent collision. All spatial and dynamic parameters were consistently scaled with reference to the intrinsic NL volumetric unit. We monitored online relevant parameters and statistics, such as *e.g.* detailed assembly history and agent velocity distribution. In absence of gravity and fluidic drag, the agent velocity distribution assumed (at least qualitatively) a Maxwellian profile after sufficiently-long simulation times (independently of the initial speed magnitude), as expected from the perfect gas-like collision mechanics encoded.

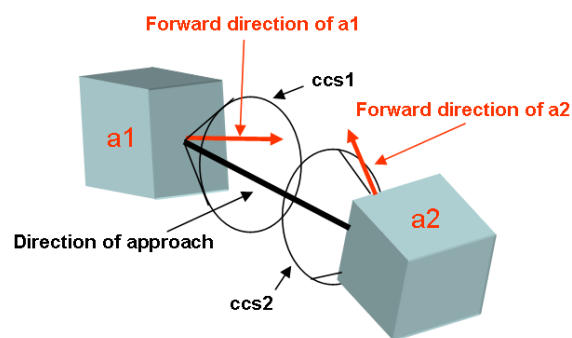


**Figure 3.** Matching capture cross-section (MCCS) criterion for effective (*i.e.* leading to self-assembly) inter-agent collisions. Each of the two colliding agents ( $a_1$  and  $a_2$ ) has a predefined CCS with respect to the direction of mutual approach. If, at the time of collision, the instantaneous movement direction of either agent is outside its own CCS (as for  $a_2$ , in this case), the collision does not lead to assembly.

We used our agent-based model to investigate the effects of several parameters and assembly strategies on FSA yield. We adopted the data from the 3D FSA process experimentally demonstrated by Zheng and Jacobs [4] to test and tune our model, and as a reference to which to compare our predictions (see Section 3).

Our model can encode all boundary conditions known for a given process to be simulated. Therefore, when all these conditions are accordingly set our model can fit actual experimental data using in principle a single parameter, *i.e.* either the probability of effective collision or each agent's capture cross-section (CCS). This single parameter may be related to the "single-component-single-carrier" capture time defined by Zheng and Jacobs in their original model [4].

<sup>1</sup> NetLogo is available at: <http://ccl.northwestern.edu/netlogo/>

### 3. RESULTS

#### Full-scale Zheng and Jacobs' 3D FSA process

Figure 4 compare simulated and experimental data, respectively, for the actual 3D FSA process of Zheng and Jacobs for the case with equal numbers of LEDs and carriers (= 100). All agent and assembly space parameters reflected as much as possible the known experimental conditions; we assumed an initial agent velocity (not measured by the experimenters) of 100 mm/s. Fig. 4a shows assembly histories for 3 values of the parameter  $\theta$ , that in the MCCS criterion describes each agent's CCS as a solid angle of  $2\pi(1 - \cos(\theta/2))$ . As expected, larger CCSs lead to faster assembly;  $\theta = 80^\circ$  closely fits experimental data.

#### Investigations: agent redundancy and density

In a 10x consistently-downscaled version of the full-scale system (to reduce computation time), we simulated the effects of redundancy (*i.e.* of LEDs-to-carriers ratio; Fig. 5a) and of assembly space-to-component volume ratio (Fig. 5b) on assembly rates. Both higher redundancy and smaller space-to-component volume ratio increase assembly rates.

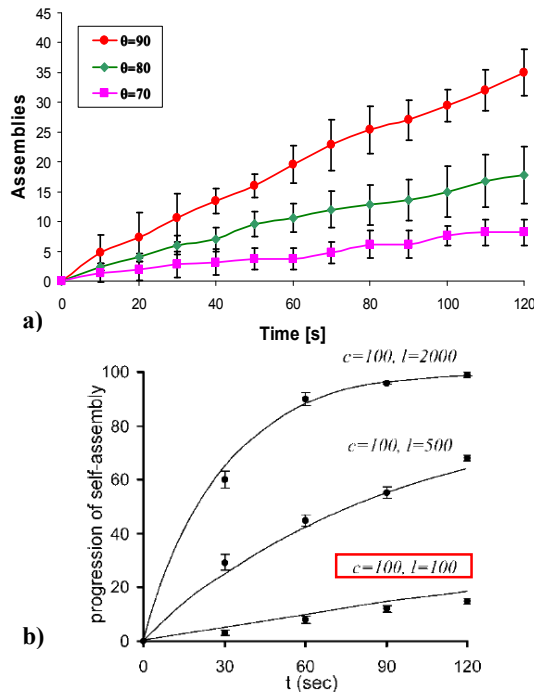


**Figure 4.** ABM of Zheng and Jacobs' 3D FSA process. **a)** Full-scale simulations (assembly space volume:  $4394 \text{ mm}^3$ , 100 LEDs + 100 carriers, initial agent speed: 100 mm/s) using the capture cross-section as the only fitting parameter (averages and standard deviations of 5 histories shown for each CCS value). A CCS defined by  $\theta = 80^\circ$  can match the experimental data, reproduced in **b)** (LEDs ( $l$ ) = carriers ( $c$ ) = 100; from [4], courtesy of H. O. Jacobs).

#### Investigations: assembly strategies

So far, in all simulated FSA processes, given the initial conditions, populations of agents evolved according to actual assembly events only. This does

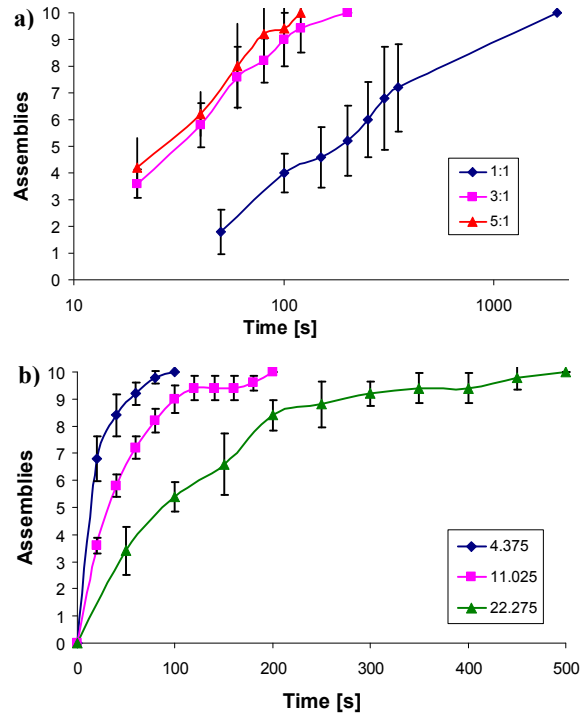


**Figure 5.** ABM investigations on a 3D FSA downscaled system (reference model: 10 + 10 agents; 10x smaller assembly space; 100 mm/s initial speed; assembly criterion: MCCS with  $\theta = 80^\circ$ ). Larger redundancy (*i.e.* LEDs-to-carriers ratio, here ranging from 1:1 to 5:1) increases the assembly rate **(a)**, as well as a smaller space-to-agent volume ratio (here ranging from 4 to 11 and 22)**(b)**. Averages and standard deviations of 5 histories shown for each parameter.

not necessarily need to be so: agent populations may be externally supplied with more of their own agents during the assembly process, *e.g.* according to predefined strategies. We investigated the effects on assembly rates of feeding strategies on the downscaled FSA system. We devised 3 basic strategies subjected to the constraint of constant total number of agents in the (fixed) assembly space. Specifically, at the very time of every assembly event, a new component was added which was: for the "red-up" strategy, an LED; for "alter", alternatively a carrier and a LED; for "red-down", a carrier. Furthermore, we set out to investigate the role of assembled (thus inert) parts: do they work as catalysts or barriers for unassembled agents? For this, we devised a strategy ("As-out") where assemblies were removed from the assembly space as soon as they formed (*i.e.* assembly led to agent annihilation).

Fig. 6 shows the results for the simulated strategies. All feeding strategies increased the assembly rate as compared to the standard ("none") case. Moreover, feeding LEDs (*i.e.* increasing redundancy at run time and as compared to initial agent populations) has larger positive effects on the assembly rates, as compared to feeding carriers. Also, our preliminary results hint at a barrier (catalyst) role for assemblies during the initial (final) stages of the processes, as evidenced in comparison with the ordinary case. This is however not yet clear, and object of current studies.

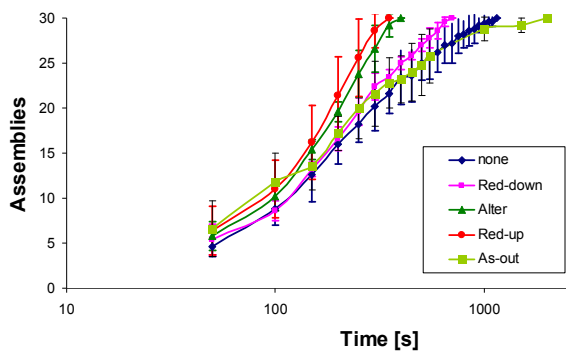


**Figure 6.** ABM investigations on assembly strategies. External feeding of agents during assembly significantly affects assembly rates. Assembled agents may work as catalysts and barriers in the first and last stages of the process, respectively (initial and boundary conditions: assembly space:  $5 \times 5 \times 5 \text{ mm}^3$ ; 60 LEDs + 30 carriers; initial agent velocity: 100 mm/s; assembly criterion: MCCS with  $\theta = 80^\circ$ ). Averages and standard deviations of 5 histories shown for each strategy.

#### ABM of a sequential 3D FSA process

Finally, we used our model to predict the behavior of a hypothetical, sequential 3D FSA process involving 3 sets of agents *co-existing* in the assembly space. The corresponding, constrained assembly sequence was:  $(a1+a2) + a3 \rightarrow as1 + a3 \rightarrow as2$ , as sketched in Fig. 7a. Simulations of the proposed process (Fig. 7b) indicated that *as2*'s should increase exponentially, as for a single-step assembly process, while *as1*'s should progress in a non-monotonic way, whose details sensibly depend on agents' relative abundance and probability of effective collision. Yield of reaction- and diffusion-limited processes may thus be compared.

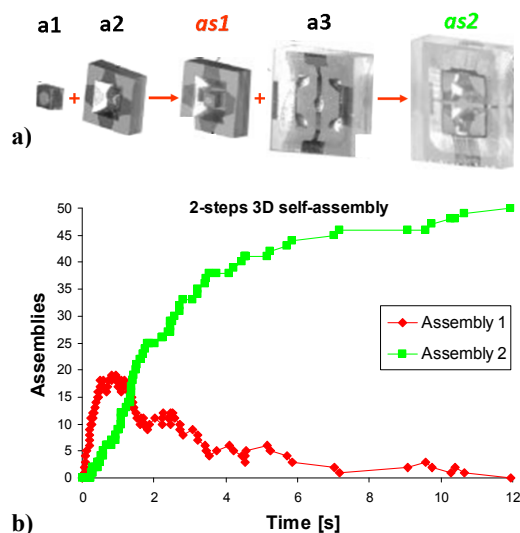


**Figure 7.** Hypothetical sequential 3D FSA process. **a)** All agents (*a1* to *a3*) present in the assembly space at starting time (illustration elaborated from [4], courtesy of H. O. Jacobs). **b)** Simulated assembly history (initial populations: 50 *a1*, 100 *a2*, 100 *a3*; initial agent velocity: 100 mm/s; assembly space:  $15 \times 15 \times 15 \text{ mm}^3$ ; assembly criterion: probabilistic with effective collision probability of 25%).

#### 4. CONCLUSIONS

We present ABM as a natural framework to numerically explore MEMS FSA's vast parameter space and to elucidate its standing issues – including *e.g.* scaling, collective phenomena and assembly strategies. These represent some of the critically important tasks for a deeper understanding and wider appreciation of FSA processes.

Our ABM implementation is computationally expensive: for each simulation run, NL stores each agent's degrees of freedom, velocity components and set of neighboring agents. Also, it constitutes only a geometrical approximation of actual (F)SA processes. As a long-term perspective, we envision implementing the assembly physics and dynamics with physical engines embedded in object-oriented codes. This might radically increase realism and match with experimental details while possibly reducing the simulation time.

#### ACKNOWLEDGMENTS

M.M. thanks the Santa Fe Institute and the CSSS09ers for inspiration. K.B. and R.S. were partly funded by the Center on Interfacial Engineering for Microelectromechanical Systems (CIEMS) under DARPA grant HR0011-06-0049 (Dr. D. L. Polla, Program Manager) and by Intel Corporation.

#### REFERENCES

1. M. Mastrangeli, S. Abbasi, C. Varel, C. Van Hoof, J.-P. Celis and K. F. Böhringer, "Self-assembly from milli- to nanoscales: methods and applications", *J. Micromech. Microeng.*, vol. 19, 083001 (37 pp), 2009
2. S. A. Stauth and B. A. Parviz, "Self-assembled single-crystal silicon circuits on plastic" *Proc. Nat. Acc. Sc.*, vol. 103, no. 38, pp. 13922-7, 2006
3. W. Zheng and H. O. Jacobs, "Self-Assembly Process to Integrate and Connect Semiconductor Dies on Surfaces with Single-Angular Orientation and Contact-Pad Registration", *Adv. Mater.*, vol. 18., pp. 1387-1392, 2006
4. W. Zheng and H. O. Jacobs, "Fabrication of multicomponent microsystems by directed three-dimensional self-assembly", *Adv. Funct. Mater.*, vol. 15. no.5, pp. 732-8, 2005
5. A. K. Verma, M. A. Hadley, H.-J. J. Yeh, J. S. Smith, "Fluidic self-assembly of silicon microstructures", *Proc. ECTC*, 1995.
6. E Klavins, S. Burden and N. Napp, "Optimal Rules for Programmed Stochastic Self-Assembly", in *Robotics: Science and Systems*, MIT Press, pp. 9-16, 2006
7. J. Lienemann, A. Greiner, J. G. Kornink, X. Xiong Y. Hanein and K. F. Böhringer, "Modeling, simulation and experimentation of a promising new packaging technology—parallel fluidic self-assembly of micro devices", *Sensors Update*, vol. 13, 2003
8. D. Gillespie, Stochastic simulation of chemical kinetics, *Annual Review of Physical Chemistry*, vol. 58, pp. 35-55, 2007
9. G. Mermoud, J. Brugger and A. Martinoli, "Toward multi-level modeling of self-assembling intelligent micro-systems", *Proc. Int. Conf. on Autonomous Agents and Multiagent Systems*, pp. 89-96, 2009
10. M. Luck, R. Ashri and M. D'Inverno, *Agent-based software development*, Artech House, 2004
11. E. Sklar, "Software review: Netlogo, a multi-agent simulation environment", *Artificial Life*, vol. 13, no.3, pp. 313-311, 2007